arXiv:cond-mat/0602519v1 [cond-mat.mtrl-sci] 22 Feb 2006

In Search of Microscopic Evidence for Molecular Level Negative Thermal Expansion in Fullerenes

S. Brown[1],[*] J. Cao[1], J. L. Musfeldt[1], N. Dragoe[2], F. Cimpoesu[3], S. Ito[4], H. Takagi[4], and R. J. Cross[5]
[1]*Department of Chemistry, University of Tennessee, Knoxville, Tennessee 37996-1600*
[2]*ICMMO - LEMHE, Université Paris XI, Bat 410, UMR 8647-CNRS, Orsay 91405, France*
[3]*Institute of Physical Chemistry, Splaiul Independentei 202, Bucharest 77208, Romania*
[4]*Department of Advanced Materials Science, University of Tokyo,*
Kashiwa-no-ha 5-1-5 Kibanto 403, Kasiwa 277-8561, Japan and
[5]*Department of Chemistry, Yale University, PO Box 208107, New Haven, Connecticut 06520-8107*
(Dated: February 6, 2008)

We report the high-resolution far infrared vibrational properties of C_{60} and endohedral Kr@C_{60} fullerene as a function of temperature. Anomalous softening of the $F_{1u}(1)$ mode (526 cm^{-1}) is observed throughout the temperature range of investigation (300 - 10 K) suggesting that the fullerene cage may expand at low temperature in these molecular solids. To test this idea, we combine these results with temperature and pressure dependent Raman, infrared, and Kr extended x-ray absorption fine structure data from the literature to provide a comprehensive view of local cage size effects. The results are consistent with a recent molecular dynamics study [Kwon *et al.*, Phys. Rev. Lett. **92**, 15901 (2004)] that predicts negative thermal expansion in carbon fullerenes.

PACS numbers: 61.48.+c, 78.30.-j, 65.40.-b, 63.20.-e

INTRODUCTION

The interplay between thermal, mechanical, and vibrational properties that gives rise to negative thermal expansion (NTE) in complex materials is an area of sustained scientific interest. ZrW_2O_8 is a prime example, where bulk NTE is present over a wide temperature range and is attributed to unusual low-frequency dynamics [1, 2, 3, 4]. Various layered and molecular solids exhibit similar behavior although the mechanisms driving NTE can be different. For instance, graphite and related layered solids display anisotropic negative thermal expansion even well above room temperature [5, 6]. In graphite, NTE is primarily due to the intra-layer tension effect, whereas in molecular solids such as $Sm_{2.72}C_{60}$, NTE originates from the mixed electronic configuration of Sm [7]. Based on bonding pattern similarities and compressibility arguments, it has been anticipated that other nanocarbon materials (including fullerenes, small cage compounds, and nanotubes) may also exhibit unusual properties [8]. Independent of the many scientific discoveries in this area, the technological dream is to exploit negative and zero expansion materials in composites and molecular electronics devices that have specifically tailored thermal expansion coefficients.

A number of recent molecular dynamics simulations have focused on the thermal properties of small cage fullerenes and carbon nanotubes [8, 9, 10, 11]. Of particular interest is the molecular dynamics investigation by Kwon *et al.*, which predicted NTE in C_{60} up to moderate temperatures due to an unusual combination of structural and vibrational entropic effects [8]. The calculated value of the maximum volumetric thermal expansion coefficient is -1×10^{-5} K^{-1} [8], comparable to that in ZrW_2O_8 [2]. It is important to note that NTE in C_{60} is predicted to be a molecular-level rather than bulk effect [8]. As a consequence, local or "microscopic" probes are required to investigate this prediction. At this time, theoretical results for carbon nanotubes are more controversial [8, 9, 10, 11], demonstrating the need for additional work in this area.

At ambient temperature and pressure, C_{60} fullerene has the shape of a truncated icosahedron (point group I_h) with 12 pentagonal and 20 hexagonal faces. It displays both long (between a hexagon and a pentagon, l= 1.45 $\AA$) and short (between hexagons, l= 1.40 $\AA$) bonds [12]. Due to the high point symmetry, isolated C_{60} molecules display 46 distinct vibrational modes. Of this set, $4F_{1u}$ are infrared active, and $2A_g$ + 8 H_g are Raman active. These modes can be differentiated by the percentage of radial and tangential displacement of molecule in a particular vibrational mode [13]. For example, $F_{1u}(1)$ and $F_{1u}(2)$ modes are 93.5 and 66.6% radial while $F_{1u}(3)$ and $F_{1u}(4)$ are 48.7 and 99.5% tangential in character, respectively [13, 14]. In the solid state, C_{60} molecules crystallize in face-centered cubic arrangement with space group $Fm\bar{3}m$ ($O_h{}^5$) [15]. The room temperature phase is orientationally disordered due to rapid and continuous rotation of the C_{60} icosahedra [16]. C_{60} undergoes a first-order structural transition to a simple cubic structure ($Pa\bar{3}/T_h{}^6$) at 260 K and to an orientationally ordered phase at around 90 K [17, 18, 19]. Bulk structural studies show that lattice parameter trends are standard over the full temperature regime (Table I) [20].

Incorporation of a noble gas atom such as Kr inside the cage leads to a stable endohedral fullerene (Kr@C_{60}) with an average Kr-C separation of 3.540(3) Å [24, 25]. Comparison of this distance with the sum of the van der Waals

TABLE I:
Structural studies of crystalline C_{60} fullerene.

T (K)	a (Å)	Ref.	P (GPa)	a (Å)	Ref.
270	14.1543(2)	[21]	0.35(5)	14.067(2)	[23]
170	14.0708(1)	[21]	0.41(5)	14.031(5)	[23]
110	14.052(5)	[22]	0.55(5)	13.978	[23]
11	14.04(1)	[19]	2.4(1)	13.730	[23]
5	14.0408(1)	[17]	2.5(1)	13.633	[23]

radii for carbon and krypton (3.72 Å) demonstrates that the Kr atom is tightly confined within the surrounding cage. Recent synchrotron x-ray diffraction work on the similar Ar@C_{60} indicates that the unit cell parameter is slightly larger than that of C_{60} at 300 K and slightly smaller at low temperature [26].

It is clearly of great interest to compare the theoretical predictions for molecular level NTE in small cage fullerenes with experimental observations. In this article, we report a high-resolution far infrared study of C_{60} and Kr@C_{60} as a function of temperature with particular focus on the $F_{1u}(1)$ and $F_{1u}(2)$ vibrational modes. Unusual softening of the $F_{1u}(1)$ mode is observed with decreasing temperature in both compounds, consistent with predictions for an expanded low temperature fullerene ball. To further test this idea, we combine our results with previous structural and vibrational studies (including variable temperature and pressure Raman, infrared, and Kr extended x-ray absorption fine structure data [25, 27, 28, 29, 30, 31, 32, 33, 34, 35, 36, 37]) to evaluate mode Grüneissen parameters and elucidate the thermal expansion coefficient of C_{60}. Many of the mode Grüneissen parameters are negative, and we estimate that α_{vib} is on the order of -10^{-5} K^{-1}. We also discuss the subtle guest-host interaction in Kr@C_{60}.

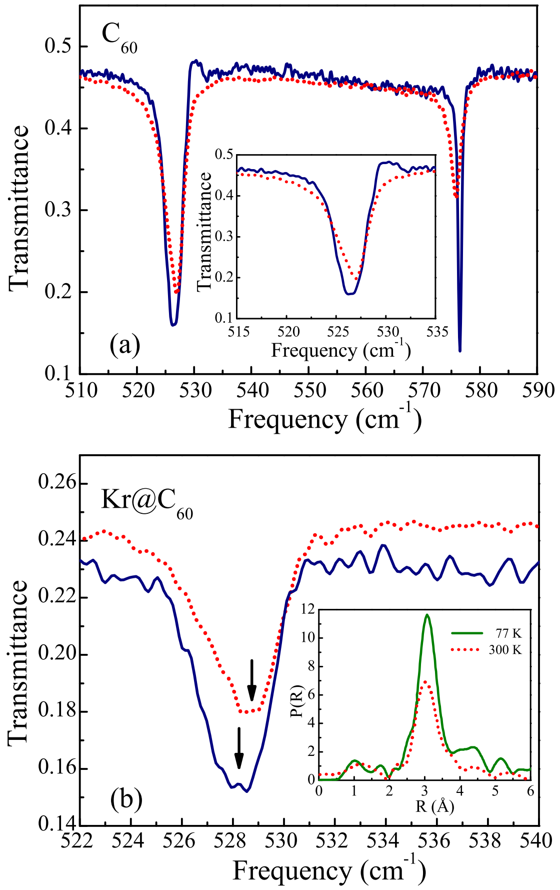

FIG. 1: (Color online) (a) High resolution far infrared transmittance spectra of C_{60}. Note that the $F_{1u}(1)$ mode splits and softens at low temperature, whereas the $F_{1u}(2)$ mode hardens. The inset shows a close-up view of $F_{1u}(1)$ mode softening. (b) Close-up view of the low temperature $F_{1u}(1)$ mode softening in Kr@C_{60}. The inset displays previous Kr-EXAFS results [25]. In all panels, the red (dotted) lines represent 300 K results, whereas the blue (solid) lines correspond to 4 K data. In the inset, the green (solid) line corresponds to 77 K data.

METHODS

Endohedral fullerenes were synthesized using the high-pressure, high-temperature technique described earlier [25]. The resulting product contained both C_{60} powder and ∼1% Kr@C_{60}. Multiple separations were carried out using a Jasco Gulliver 1500 high-performance liquid chromatography system, equipped with recycling, automatic injection, and a diode array detector (300 - 900 nm). Using a detailed procedure involving recycling and sequential chromatography [25], about 1 mg of 99% pure Kr@C_{60} was obtained. The pristine C_{60} used in this work was obtained from Aldrich (99.9% purity).

Variable temperature far infrared transmittance measurements were performed using a Bruker 113V Fourier transform infrared spectrometer, covering the frequency range from 22 - 650 cm^{-1} with both 0.1 and 0.5 cm^{-1} resolution. A helium-cooled bolometer detector was employed for added sensitivity. The measurements were done using isotropic, pressed pellets (∼1% by weight) with paraffin as the matrix material. Low temperature spectroscopies were carried out with a continuous-flow helium cryostat and temperature controller. Standard peak fitting techniques were employed, as appropriate.

RESULTS AND DISCUSSION

Figure 1 shows the far infrared transmittance spectra of fullerene C_{60} and Kr@C_{60} at 10 and 300 K. For C_{60}, the radial $F_{1u}(1)$ and $F_{1u}(2)$ modes are observed at 526 and 576 cm^{-1}, consistent with previous work [38]. The most striking result is the temperature dependence of the

$F_{1u}(1)$ mode, which softens by $\sim$0.5 cm^{-1} with decreasing temperature. This effect occurs gradually throughout the entire temperature range. Note that the fine structure in $F_{1u}(1)$ is a result of crystal field symmetry breaking below the 260 K transition and was investigated in detail by Homes *et al.* [38]. At low temperature, F_{1u} splits as $F_{1u} \rightarrow A_u + E_u + 3F_u$, of which only the F_u modes are infrared active [39, 40]. The unusual softening of $F_{1u}(1)$ was not, however, discussed in earlier measurements. A similar softening effect appears in endohedral Kr@C$_{60}$, as shown in Fig. 1(b). Taken together, these temperature dependent mode softening trends support a more relaxed ball at low temperature. In contrast to the observed softening in $F_{1u}(1)$, the other radial mode, $F_{1u}(2)$, exhibits normal behavior, that is, hardening with decreasing temperature. The mode sharpens and grows in strength as the sample is cooled. The absence of crystal field-induced fine structure in $F_{1u}(2)$ has been previously attributed to the degree of overlap between 6:6 bond and the adjacent pentagon [42].

Figure 2 displays the peak position of the $F_{1u}(1)$ mode in pristine C$_{60}$ and Kr@C$_{60}$ as a function of temperature. Two major trends are observed. First, the $F_{1u}(1)$ mode softens throughout the measured temperature range for both C$_{60}$ and Kr@C$_{60}$. Second, the $F_{1u}(1)$ mode hardens by $\sim$2 cm^{-1} upon endohedral incorporation [43]. A hardening trend was also observed for the $F_{1u}(1)$ mode in a previous study [44]. The $F_{1u}(2)$ mode frequency in Kr@C$_{60}$ (577 cm^{-1}) is also $\sim$1 cm^{-1} higher than that in the pristine material. Noble gas-containing endohedrals are traditionally considered to be van der Waals complexes due to the inert nature of noble gas guest atom. In such a picture, only modest spectral changes (such as the appearance of a rattling mode) are anticipated upon endohedral incorporation. The observed radial mode hardening (Fig. 2) and tangential mode softening [45] in Kr@C$_{60}$ compared with pristine C$_{60}$ suggests a modest guest-host interaction and a slight modification of the encapsulant/cage interaction potential.

Returning our attention to the temperature dependent mode softening problem, a literature survey shows that a number of Raman active modes also display unexpected low temperature softening [27, 28, 29, 30]. Just to cite a few examples, van Loosdrecht *et al.* [27] observed softening of several different modes ($H_g(3)$, $H_g(4)$, $A_g(2)$ and $H_g(8)$) both above and below the 260 K transition temperature. (All modes harden at the transition temperature.) Hamanaka *et al.* showed that the $H_g(7)$ mode softens below 260 K, whereas the $A_g(2)$ mode softens below 160 K. The $H_g(3)$ and $H_g(5)$ modes remain almost unchanged with decreasing temperature [29]. In contrast, Horoyski *et al.* reported almost no change in $A_g(2)$ and $H_g(4)$ in the lower temperature range [30, 46]. Dong *et al.* observe higher order overtone and combination modes in C$_{60}$, although their exact temperature dependence is not clear [41]. Taken together, we find that several (but not all) Raman investigations support unusual low temperature vibrational mode softening.

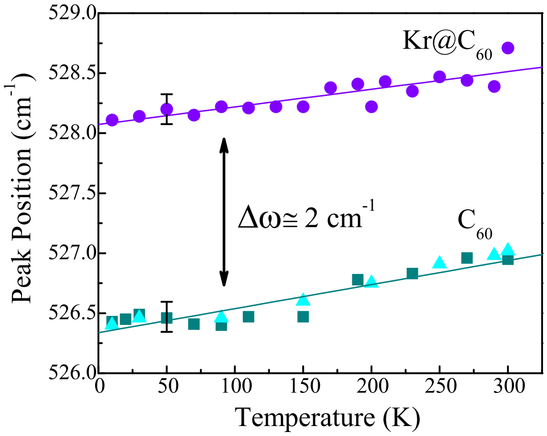

FIG. 2: (Color online) Temperature dependence of the center peak position of the $F_{1u}(1)$ mode in C$_{60}$ and Kr@C$_{60}$. The blue-shift of this mode in the endohedral material suggests modest guest-host interactions. Two independent runs are shown for C$_{60}$. Error bars are indicated.

It is of interest to understand the microscopic origin of the unusual mode softening and its implications for the bulk properties. In general, mode softening can be correlated to two major effects: volume and charge. The charge effect is well-known in organic charge transfer salts [47, 48]. Typically, volume contributions dominate in high pressure experiments. High-pressure vibrational studies, detailed below, also indicate extensive mode softening [31, 32, 33, 34, 35, 36, 37]. Hence, we attribute both pressure and temperature dependent mode softening to cage volume effects [49].

Volume change can be quantified by the thermal expansion coefficient as

$$\alpha = \frac{\gamma_{av} C_V}{V_m B} = \frac{\chi_T}{V_m} \sum_i \gamma_i c_i. \tag{1}$$

Here, B ($= 1/\chi_T$) is the bulk modulus, γ_{av} ($= \sum_i \gamma_i c_i / \sum_i c_i$) is the average of mode Grüneisen parameters γ_i weighted by the mode specific heat c_i, C_V is total molar specific heat at constant volume, and V_m is the molar volume [50]. The mode Grüneisen parameters are dimensionless quantities that relate the fractional change in volume to the fractional change in frequency of a given mode. They are defined as

$$\gamma_i = -\left(\frac{\delta \ln \omega_i}{\delta \ln V}\right) = \frac{1}{\omega_i \chi_T}\left(\frac{\delta \omega_i}{\delta P}\right), \tag{2}$$

where ω_i is the frequency of the i^{th} mode. At high temperatures, the γ_{av} can be taken as the arithmetic mean of mode Grüneisen parameters γ_i. Note that thermal expansion will be positive or negative depending upon whether positive or negative γ_i predominate in the weighted average [3, 4, 50].

To evaluate these quantities, we examined the pressure dependent vibrational properties data that are available in the literature. Meletov *et al.* measured the Raman spectrum of C_{60} between 200 - 800 and 1350 - 1700 cm^{-1} [31, 51]. The results clearly show three well-defined phases: below 0.4 GPa, between 0.4 and 2.4 GPa, and above 2.4 GPa. These pressure-induced phase transitions are attributed to orientational ordering from face-centered cubic to a simple cubic structure and finally to a rotation-free orientationally-ordered simple cubic phase in the high pressure regime [31]. Comparison of lattice parameter trends with temperature and pressure (Table I) demonstrates the rationale for concentrating our analysis on the pressure range below 0.4 GPa, although to obtain the fullest possible mode contributions, we also employ higher pressure results in our secondary analysis, below. Returning to the data of Meletov *et al.* [31], almost all the modes soften up to 0.4 GPa, whereas $H_g(3)$, $H_g(4)$ soften through the higher pressure range as well. Similar softening has been observed for the $A_g(2)$ mode at 0.35 GPa [32]. Further, Snoke *et al.* showed that the $F_{1u}(1)$, $H_g(3)$, and $H_g(4)$ modes soften up to 14 GPa [33]. Unusual softening of $F_{1u}(1)$ and several Raman and infrared inactive modes are also observed in other independent variable pressure measurements [34, 35, 36, 37]. Martin *et al.* highlight pressure-induced softening of many inactive modes up to 2.5 GPa as well [35]. Despite these experimental findings, no comprehensive explanation for the unusual mode softening of $F_{1u}(1)$ and the aforementioned Raman active modes has been advanced [52].

Table II summarizes our extended analysis of the aforementioned pressure dependent vibrational studies of C_{60}, undertaken as part of our search for microscopic evidence of molecular level NTE in fullerenes. As discussed previously, many modes soften with increasing pressure (especially between 0 - 0.4 GPa), giving negative Grüneisen parameters for the majority of modes. The size and sign of the Grüneisen parameters are compatible with small but significant expansion in intramolecular bond lengths as pressure is increased or temperature is decreased [49]. Also, note that both radial and tangential modes exhibit pressure-induced softening [55]. The average value of the mode Grüneisen parameters including most of optically active modes (upper portion, Table II) is negative in this pressure range (γ_{av} ∼ -0.19). In order to further pin point the total average mode Grüneisen parameter for C_{60}, we extended this analysis to include several optically inactive and two Raman active modes over a somewhat larger pressure range 0.5 - 2.5 GPa [35]. The selected modes are shown in the lower portion of Table II. Thus, combining the data for these modes in the higher pressure range (0.5 - 2.5 GPa) with the aforementioned mode Grüneisen parameter of the optically active modes in the lower pressure range yields an averaged value of the mode Grüneisen parameter that is also negative (γ_{av} ∼ -0.10).

TABLE II:

Mode Grüneisen parameters of the Raman, infrared active, and inactive modes of C_{60} in two different pressure ranges: 0 - 0.4 and and augmented to include selected data from 0.5 - 2.5 GPa. The reported value of $\chi_T = 6.9 \times 10^{-2}$ GPa^{-1} is used in the calculation [54].

Mode	ω (cm^{-1})	dω/dP (cm^{-1}/GPa)	Ref.	γ_i
$H_g(1)$	272	-15.00	[31]	-0.80
$H_g(2)$	435	-12.00	[31]	-0.40
$A_g(1)$	496	-12.00	[31]	-0.35
$F_{1u}(1)$	526	-1.60	[37]	-0.04
$F_{1u}(2)$	576	2.40	[37]	0.06
$H_g(3)$	710	-12.00	[31]	-0.24
$H_g(5)$	1099	-	[31][a]	-
$F_{1u}(3)$	1182	3.90	[37]	0.05
$H_g(6)$	1248	-	[31][a]	-
$F_{1u}(4)$	1429	6.10	[37]	0.06
$A_g(2)$	1467	-18.00	[31]	-0.18
$H_g(8)$	1570	-7.00	[31]	-0.06
				γ_{av} ∼ -0.19[b]
$H_g(4)$	772	-2.70	[36][c]	-0.05
$H_g(7)$	1422	9.80	[36][c]	0.10
$H_u(3)$	668	0.62	[35][c]	0.01
$F_{2u}(2)$	712	-1.70	[35][c]	-0.04
$G_u(2)$	741	-1.90	[35][c]	-0.04
$F_{2u}(3)$	796	0.73	[35][c]	0.01
$H_u(4)$	824	3.00	[35][c]	0.05
$G_g(2)$	961	1.80	[35][c]	0.03
				γ_{av} ∼-0.10[d]

[a] Ref. [51]

[b] Low pressure regime: 0 - 0.4 GPa.

[c] Slope between 0.4 - 2.4 GPa

[d] Inclusion of Raman and infrared active modes from the low pressure regime as well as selected inactive modes with pressure-dependent frequency shifts obtained from the high pressure regime, as indicated in the Table.

Can we use this information to calculate the thermal expansion coefficient, α? Certainly, the negative value of the averaged Grüneisen parameter is directly related to a negative thermal expansion coefficient. With precise knowledge of mode Grüneisen parameters and phonon densities of states for each mode, the calculation of thermal expansion coefficient is straightforward (Eqn. (1)). It is, however, important to point out that isolated C_{60} has 46 vibrational modes and that we are able to evaluate Grüneisen parameters for only a small subset based upon currently available data, despite the two different trials presented in Table II. To finesse this problem, we designate α_{vib} as the vibrational part of the thermal expansion coefficient for the optically-active modes in the low pressure range (0 - 0.4 GPa) shown in Table II. Using the reported density of states [56, 57], each mode was weighted to calculate the total specific heat from mode specific heat and finally our pseudo thermal expansion coefficient, α_{vib} [4]. Based upon this data, we find α_{vib} to be on the order of -10^{-5} K^{-1}. Inclusion of the inactive modes over the larger pressure range (bottom portion of Table II) does not modify this general picture. Note that this value quantifies molecular rather than conventional lattice effects.

Independent experimental support for this vibrational analysis and the predictions of Kwon *et al.* [8] comes from our reanalysis of the extended x-ray absorption fine structure study of Kr@C_{60}, performed at the Kr-edge of the encapsulated Kr atom at 77 and 300 K [25]. X-ray absorption spectroscopy is a sensitive and direct probe of molecular size and other local effects. The inset of Fig. 1(b) shows the Kaiser-Bessel Fourier transformed data. A small shift in the peak position (to higher values of R) is clearly evident at low temperature and is consistent with the mode softening of various infrared and Raman active modes. The Fourier analysis and fitting is tricky, but the authors extract a Kr-C path distance of 3.540(7) Å at low temperature and 3.537(10) Å at 300 K, indicating the possibility of a slightly relaxed low temperature cage [58]. Translating this observation into a thermal expansion coefficient, we obtain on the order of -10^{-5} K^{-1}, similar to that extracted from our vibrational analysis.

Combined, these experiments provide broad support for the proposed molecular-level NTE in small carbon cage compounds. In C_{60} and Kr@C_{60}, selected modes soften as temperature is lowered and/or pressure is increased. The mode softening correlates directly with the size and geometry of the fullerene cage and NTE at molecular level offers a universal explanation of both temperature and pressure effects [8, 55]. The trend holds even in the presence of subtle guest-host interactions in Kr@C_{60}. As discussed by Kwon *et al.* [8], low-temperature cage expansion may originate from an unusual combination of structural and vibrational entropic effects. Hence, NTE may be an intrinsic property of fullerene and other small-cage molecules, although in bulk measurements, the molecular-level effect may be dominated by bulk lattice expansion. On the other hand, molecular electronics applications exploit single molecular properties. Understanding the thermal properties of functional, assembled molecular-based materials presents many future opportunities and challenges.

CONCLUSION

We report the the high-resolution far infrared vibrational properties of C_{60} and Kr@C_{60}. We observe that the $F_{1u}(1)$ mode softens with decreasing temperature in both materials (300 - 10 K) and propose that the softening is correlated to low temperature expansion of fullerene cage. This finding is consistent with previous temperature/pressure dependent vibrational spectroscopy and is also supported by our reanalysis of temperature dependent Kr extended x-ray absorption fine structure data [25, 27, 28, 29, 30, 31, 32, 33, 34, 35, 36, 37]. To further test this hypothesis, high pressure spectral results [31, 36, 37] were employed to calculate the mode Grüneisen parameters. Many of these Grüneisen parameters are negative. These results are consistent with the recent prediction for molecular-level NTE by Kwon *et al.* [8]. Further work is needed to extend these ideas to doped fullerenes and other curved molecular systems.

ACKNOWLEDGEMENTS

This project was supported by the US National Science Foundation under Grant No. DMR-01394140 (UT) and No. CHE-0307168 (YU). We thank D. Tománek and Y.-K. Kwon for valuable discussions.

---

* Electronic address: brown@ion.chem.utk.edu

[1] J. N. Hancock, C. Turpen, and Z. Schlesinger, G. R. Kowach, A. P. Ramirez, Phys. Rev. Lett. **93**, 225501 (2004).

[2] T. A. Mary, J. S. O. Evans, T. Vogt, and A. W. Sleight, Science **272**, 90 (1996).

[3] G. Ernst, C. Broholm, G. R. Kowach, and A. P. Ramirez, Nature **396**, 147 (1998).

[4] T. R. Ravindran, A. K. Arora, and T. A. Mary, Phys. Rev. Lett. **84**, 3879 (2000).

[5] G. D. Barrera, J. A. O. Bruno, T. H. K. Barron and N. L. Allan, J. Phys.: Condens. Matt. **17**, R217 (2005).

[6] J. B. Nelson, And D. P. Riley, Proc. Phys. Soc. London **57**, 477 (1945).

[7] J. Arvanitidis, K. Papagelis, S. Margadonna, K. Prassides, and A. N.Fitch, Nature **425**, 599 (2003).

[8] Y.-K. Kwon, S. Berber, and D. Tománek, Phys. Rev. Lett. **92**, 015901 (2004).

[9] C. Li, and T.-W. Chou, Phys. Rev. B **71**, 235414 (2005).

[10] H. Jiang, B. Liu, Y. Huang, and K. C. Hwang, J. Eng. Mater. Technol. **126**, 265 (2004).

[11] P. K. Schelling, and P. Keblinski, Phys. Rev. B **68**, 035425 (2003).

[12] C. S. Yannoni, P. P. Bernier, D. S. Bethune, G. Meijer, and J. R. Salem, J. Am. Chem. Soc. **113**, 3190 (1991).

[13] R. E. Stanton, and M. D. Newton, J. Phys. Chem. **92**, 2141 (1988).

[14] Four infrared active modes are $F_{1u}(1)$, $F_{1u}(2)$, $F_{1u}(3)$ and $F_{1u}(4)$ at 526, 576, 1182 and 1429 cm^{-1} respectively.

[15] P. A. Heiney, G. B. M. Vaughan, J. E. Fischer, N. Coustel, D. E. Cox, J. R. D. Copley, D. A. Neumann, W. A. Kamitakahara, K. M. Creegan, D. M. Cox, J. P. McCauley Jr., and A. B. Smith III, Phys. Rev. B **45**, R4544 (1992).

[16] C. S. Yannoni, R. D. Johnson, G. Meijer, D. S. Bethune, and J. R. Salem, J. Phys. Chem. **95**, 9 (1991).

[17] W. I. F. David, R. M. Ibberson, J. C. Matthewman, K. Prassides, T. J. S. Dennis, J. P. Hare, H. W. Kroto, R. Taylor, and D. R. M. Walton, Nature **353**, 147 (1991).

[18] R. Sachidanandam, and A. B. Harris, Phys. Rev. Lett. **67**, 1467 (1991).

[19] P. A. Heiney, J. E. Fischer, A. R. McGhie, W. J. Romanow, A. M. Denenstein, J. P. McCauley Jr., A. B. Smith III, and D. E. Cox, Phys. Rev. Lett. **66**, 2911 (1991).

[20] The lattice parameter increases by 0.044 ± 0.004 Å near the 260 K transition [15].

[21] W. I. F. David, R. M. Ibberson, and T. Matsuo, Proc. R. Soc. London A **442**, 129 (1993).

[22] S. Z. Liu, Y.-J. Lu, M. M. Kappes, and J. A. Ibers, Science **254**, 408 (1991).

[23] A. P. Jephcoat, J. A. Hriljac, L. W. Finger, and D. E. Cox, Europhys. Lett. **25**, 429 (1994).

[24] H. M. Lee, M. M. Olmstead, T. Suetsuna, H. Shimotani, N. Dragoe, R. J. Cross, K. Kitazawa, and A. L. Balch, Chem. Commun. **13**, 1352 (2002).

[25] S. Ito, A. Takeda, T. Miyazaki, Y. Yokoyama, M. Saunders, R. J. Cross, H. Takagi, P. Berthet, and N. Dragoe, J. Phys. Chem. B **108**, 3191 (2004).

[26] A. Takeda, Y. Yokoyama, S. Ito, T. Miyazaki, H. Shimotani, K. Yakigaya, T. Kakiuchi, H. Sawa, H. Takagi, K. Kitazawa, and N. Dragoe, Chem. Comm. (In Press).

[27] P. H. M. van Loosdrecht, P. J. M. van Bentum, and G. Meijer, Phys. Rev. Lett. **68**, 1176 (1992).

[28] M. Matus, and H. Kuzmany, Appl. Phys. A **56**, 241 (1993).

[29] Y. Hamanaka, M. Norimota, S. Nakashima, and M. Hangyo, J. Phys.: Condens. Matt. **7**, 9913 (1995).

[30] P. J. Horoyski, M. L. W. Thewalt, and T. R. Anthony, Phys. Rev. Lett. **74**, 194 (1995).

[31] K. P. Meletov, D. Christofilos, S. Ves, and G. A. Kourouklis, Phys. Rev. B **52**, 10090 (1995).

[32] N. Chandrabhas, M. N. Shashikala, D. V. S. Muthu, A. K. Sood, and C. N. R. Rao, Chem. Phys. Lett. **197**, 319 (1992).

[33] D. W. Snoke, Y. S. Raptis, and K. Syassen, Phys. Rev. B **45**, R14419 (1992).

[34] K. Aoki, H. Yamawaki, Y. Kakudate, M. Yoshida, S. Usuba, H. Yokoi, S. Fujiwara, Y. Bae, R. Malhotra, and D. Lorents, J. Phys. Chem. **95**, 9037 (1991).

[35] M. C. Martin, X. Du, J. Kwon, and L. Mihaly, Phys. Rev. B **50**, R173 (1994).

[36] K. P. Meletov, G. A. Kourouklis, D. Christofilos, and S. Ves, JETP **81**, 798 (1995).

[37] Y. Huang, D. F. R. Gilson, and I. S. Butler, J. Phys. Chem. **95**, 5723 (1991).

[38] C. C. Homes, P. J. Horoyski, M. L. W. Thewalt, and B. P. Clayman, Phys. Rev. B **49**, R7052 (1994).

[39] The low temperature space group is Pa$\bar{3}$.

[40] The natural abundance of ^{13}C reduces symmetry even further [41].

[41] Z.-H. Dong, P. Zhou, J. M. Holden, P. C. Eklund, M. S. Dresselhaus, G. Dresselhaus, Phys. Rev. B **48**, R2862 (1993).

[42] L. R. Narasimhan, D. N. Stoneback, A. F. Hebard, R. C. Haddon, and C. K. N. Patel, Phys. Rev. B **46**, 2591 (1992).

[43] Additional modes (291, 437, 602 cm^{-1}) also appear in the infrared response of Kr@C$_{60}$.

[44] K. Yamamoto, M. Saunders, A. Khong, R. J. Cross, M. Grayson, M. L. Gross, A. F. Benedetto, and R. B. Weisman, J. Am. Chem. Soc. **121**, 1591 (1999).

[45] Y. Yokoyama, S. Ito, A. Takeda, T. Miyazaki, H. Shimotani, F. Cimpoesu, N. Dragoe, H. Takagi and K. Kitazawa, Unpublished results

[46] Both studies argued that the longer wavelength excitation eliminates problems related to sample heating and photo-degradation [29, 30].

[47] R. Świetlik, K. Yakushi, K. Yamamoto, T. Kawamoto, and T. Mori, Journal of Molecular Structure **704**, 89 (2004).

[48] H. H. Wang, J. R. Ferraro, J. M. Williams, U. Geiser, and J. A. Schlueter, J. Chem. Soc.-Chem. Commun. **16**, 1893 (1994).

[49] All the modes under investigation are intramolecular modes and hence, related to cage rather than lattice effects.

[50] T. H. K. Barron, and G. K. White, *Heat Capacity and Thermal Expansion at Low Temperatures* (Kluwer Academic/Plenum Publishers, New York, 1999).

[51] The intermediate region could not be measured as it has a strong Raman mode of diamond at 1333.4 cm^{-1} which is many orders of magnitude stronger than the Raman modes of C$_{60}$.

[52] Aoki *et al.* proposed that the effect in the F_{1u} mode might be due a covalent-bond-like interaction formed between contacting faces of the adjacent molecules [34] and suggested that these intermolecular attractive force (along the radial axes) can be strengthened through the increase in the π orbital overlapping as the molecules approach each other under the application of pressure. This picture does not, however, explain tangential mode softening or hardening of the $F_{1u}(2)$ radial mode [53].

[53] B. Sundqvist, Advances in Physics, **48**, 1 (1999)

[54] J. E. Fischer, P. A. Heiney, A. R. McGhie, W. J. Romanow, A. M. Denenstein, J. P. McCauley, and A. B. Smith, Science **252**, 1288 (1991).

[55] The pressure and temperature dependent behavior of lattice parameter clearly shows that the reduction in the lattice constant at 5 K ($\sim$ 14.042 $\AA$) is already surpassed for pressure larger than 0.41 GPa ($\sim$ 14.031 $\AA$) at room temperature (Table I). Hence, we correlate the softening of modes up to 0.4 GPa in pressure to the 5 K temperature regime .

[56] K. Allen, and F. Hellman, Phys. Rev. B **60**, 11765 (1999).

[57] F. Gompf, B. Renker, H. Schober, P. Adelmann, and R. Heid, J. Supercond. **7**, 643 (1994).

[58] Note that the size of error bar is mainly due to fitting procedure. Examination of the data (inset in Fig. 1(b)) clearly shows that the peak of the radial distribution function is at a higher value of R at low temperature (77 K).